Journal of Hydrology 560 (2018) 184–201

Contents lists available at ScienceDirect

Journal of Hydrology

journal homepage: www.elsevier.com/locate/jhydrol

Research papers

Groundwater-surface water interactions across scales in a boreal landscape investigated using a numerical modelling approach

Elin Jutebring Sterte [a,c,*], Emma Johansson [b], Ylva Sjöberg [d], Reinert Huseby Karlsen [e], Hjalmar Laudon [a]

[a] Department of Forest Ecology and Management, Swedish University of Agricultural Sciences, SE-901 83 Umeå, Sweden
[b] Swedish Nuclear Fuel and Waste Management Co, Box 3091, 169 03 Solna, Sweden
[c] DHI Sweden AB, Svartmangatan 18, SE-111 29 Stockholm, Sweden
[d] Department of Physical Geography and the Bolin Centre for Climate Research, Stockholm University, SE-106 91 Stockholm, Sweden
[e] Department of Earth Sciences, Uppsala University, SE-752 36 Uppsala, Sweden

ARTICLE INFO

Article history:
Received 29 November 2017
Received in revised form 27 February 2018
Accepted 4 March 2018
Available online 06 March 2018
This manuscript was handled by P. Kitanidis, Editor-in-Chief, with the assistance of Todd C. Rasmussen, Associate Editor

Keywords:
Runoff generation
MIKE SHE
Krycklan
Water balance
Soil frost
Catchment

ABSTRACT

Groundwater and surface-water interactions are regulated by catchment characteristics and complex inter- and intra-annual variations in climatic conditions that are not yet fully understood. Our objective was to investigate the influence of catchment characteristics and freeze-thaw processes on surface and groundwater interactions in a boreal landscape, the Krycklan catchment in Sweden. We used a numerical modelling approach and sub-catchment evaluation method to identify and evaluate fundamental catchment characteristics and processes. The model reproduced observed stream discharge patterns of the 14 sub-catchments and the dynamics of the 15 groundwater wells with an average accumulated discharge error of 1% (15% standard deviation) and an average groundwater-level mean error of 0.1 m (0.23 m standard deviation). We show how peatland characteristics dampen the effect of intense rain, and how soil freeze-thaw processes regulate surface and groundwater partitioning during snowmelt. With these results, we demonstrate the importance of defining, understanding and quantifying the role of landscape heterogeneity and sub-catchment characteristics for accurately representing catchment hydrological functioning.

1. Introduction

Interactions between surface waters and groundwater are controlled by several complex and interacting processes that relate to biological and physical characteristics of the catchment, as well as intra- and inter-annual variations in climatic conditions (Knutsson and Morfeldt, 2002; Sophocleous, 2002; Woods, 2006). However, surface and sub-surface hydrological systems are commonly treated as separate components of catchments (Graham and Butts, 2005). To advance our predictive capabilities we need to consider interactions between these two hydrological systems, as demonstrated by several studies using both field-based empirical analyses (Kalbus et al., 2006; Kuraś et al., 2008; Zimmer and McGlynn, 2017) and numerical modelling (Bosson et al., 2012; Destouni, 2007; Dogrul et al., 2016; Lindgren et al., 2004; Yang et al., 2017). This requires assessments of the impact of sub-catchment heterogeneity and the partitioning of water across space and time (Brooks et al., 2012a, 2012b).

Catchment responses to inter- and intra-annual variations of climate are, in part, regulated by landscape characteristics, including variations in geology, topography and vegetation (Nippgen et al., 2011; Sivapalan, 2003; Woods, 2006). Catchment geology affects the partitioning of surface and sub-surface hydrological pathways through differences in soil porosity and the degree of soil saturation (Wu and Selvadurai, 2016), whereas local to regional topography strongly controls sub-surface flow pathways, at least in areas underlain by glacial drift (Rodhe and Seibert, 1999). In such areas, the convergence of topography is an important mechanism causing spatial gradients in soil saturation (Grabs et al., 2009). At larger scales, this results in the partitioning of water into more recent and older groundwater contributions to river discharge (Tiwari et al., 2017). Vegetation is of fundamental importance for regulating losses through evapotranspiration (ET), which varies naturally across a seasonal cycle. The effects of vegetation are clearly seen in areas experiencing deforestation, which commonly results in step increases in runoff (Andreassian, 2004), but also in areas with shallow groundwater where transpiration

* Corresponding author at: Department of Forest Ecology and Management, Swedish University of Agricultural Sciences, SE-901 83 Umeå, Sweden.
E-mail addresses: eljs@dhigroup.com (E. Jutebring Sterte), emma.johansson@skb.se (E. Johansson), ylva.sjoberg@natgeo.su.se (Y. Sjöberg), reinert.karlsen@geo.uu.se (R. Huseby Karlsen), hjalmar.laudon@slu.se (H. Laudon).

https://doi.org/10.1016/j.jhydrol.2018.03.011
0022-1694/

has been shown to strongly influence the groundwater dynamics during dry periods (Bosson et al., 2008).

Climatic conditions also play an important role in catchment hydrological responses. In high latitude environments climatic conditions such as seasonal water storage, snow melt, and frozen soils drive annual patterns in catchment hydrology (Niu and Yang, 2006). Snow depth is a major factor regulating ground temperature and consequently soil frost, as the snow cover insulates the ground from cold air temperatures during the winter (Goodrich, 1982; Hardy et al., 2001; Oni et al., 2017). Frozen soils with high soil moisture content can act as an almost impermeable layer preventing infiltration, and thaw more slowly than soils with lower water content (Brooks et al., 2012b; French, 2007; Woo, 2012). The effect of soil frost is especially important during snowmelt events, because the frozen ground allows only a limited amount of water to infiltrate and consequently produces more overland flow than with unfrozen soils (Brooks et al., 2012b; Iwata et al., 2011; Orradottir et al., 2008). Depending on soil and vegetation characteristics, the timing and potential influence of snow and soil frost processes on streamflow generation can differ between neighboring catchments with similar climates.

A common assumption in modelling runoff generation is that similar sub-catchments situated close to each other respond in similar ways to hydrological forcing. For example, one common method for estimating volumetric discharge is to use the ratio of catchment areas to scale the observed discharge from one catchment to estimate the discharge from a similar catchment without observations (Archfield and Vogel, 2010). However, as shown by Karlsen et al. (2016a,b), there can be large variability in area-specific discharge between nearby sub-catchments with seemingly similar characteristics. The specific discharge variability can range up to an order of magnitude, both on shorter and longer timescales, suggesting that adjacent catchments may function very differently. It has also been argued, that the method of studying hydrological functioning on a whole-watershed basis without process-based insights into the contributions of their parts, leaves a large gap in our understanding of surface and groundwater interactions, and of the origin of runoff contributions (Payn et al., 2012). To mechanistically describe the hydrology of catchments and enable accurate predictions of water quantity, we need to move beyond previous attempts at modelling and include sub-catchment-specific information on hydrological functioning.

To improve our conceptual and mechanistic understanding of the role of sub-catchment variability on high-latitude watershed hydrology, we quantified spatial and temporal variations in the various contributing parts, as well as including representations of some dominant winter-related processes. To do this, we used an empirically data-rich boreal catchment, the Krycklan catchment, that has available results from three decades of detailed hydrological and biogeochemical investigations from a large set of nested catchments (Laudon et al., 2013). To undertake this investigation, we used the integrated surface-sub-surface hydrological MIKE SHE model (Graham and Butts, 2005). Previously, MIKE SHE has successfully been applied in similar studies of temperate areas, where winter processes largely could be ignored (Bosson et al., 2012, 2013), and in periglacial areas (Johansson et al., 2015), where deep permafrost and active-layer processes strongly influence the catchment hydrology. However, the MIKE SHE model has not previously been applied to catchment systems where seasonal soil frost and large snow accumulation and subsequent melt must be taken into account. The main purpose of this study was to test the hypothesis that we need to consider sub-catchment characteristics, in combination with freeze-thaw processes, to explain differences in discharge and surface-groundwater flow partitioning in a northern boreal catchment.

2. Methods

2.1. General site description

Krycklan (64.23° N, 19.77° E, 67.9 km^2) is an extensively studied catchment, used for multi-disciplinary hydrology and ecology research and monitoring, in northern boreal Sweden (Laudon et al., 2013). Located in the subarctic climate zone, Kryklan has 30-year mean annual precipitation (P) and evapotranspiration (ET) of 614 mm and 303 mm, respectively (Laudon et al., 2013). Snow accumulates from late October to early May in most years, resulting in a 30-year average annual snow cover of 167 days (Laudon and Ottosson-Löfvenius, 2016).

The catchment area, which is covered to 87% by forest consisting mainly of Scots pine (Pinus sylvestris) and Norway spruce (Picea abies), spans elevations from 405 m.a.s.l. in the northwest to 114 m.a.s.l. at the outlet in the southeastern part of the catchment. The total sediment depth in the area varies between 5 and 40 m (Laudon et al., 2013). Sandy and silty tills are the dominant sediment types in the area, particulary at higher altitudes where the tills are intertwined with lakes and peatlands, which are in turn underlain by finer sediments (Fig. 1A). Due to higher hydraulic conductivity (K) in the upper part of the soil profile, the main lateral transport of groundwater is assumed to occur in the first half meter of the till (Amvrosiadi et al., 2017; Bishop et al., 2011; Ågren et al., 2014). At lower altitudes in the catchment, sandy and silty glacial deposits with high K, are the most common sediments (Fig. 1A). Small streams, both naturally-formed and man-made (to improve forest productivity during the early 20th century ditching era) connect the sub-catchments to the river network (Hasselquist and Lidberg, 2017; Kuglerová et al., 2014; Oni et al., 2015).

2.2. Input data

Based on locally-observed data and literature values on hydraulic properties (Table 2) and the conceptual model (Fig. 1C), a numerical model was established in MIKE SHE (Graham and Butts, 2005). We calibrated the MIKE SHE model based on time series of stream discharge and groundwater head data (Table 1) for the period 2009-01-01 to 2012-12-31. The MIKE SHE model consists of four compartments; overland flow (OL), stream network, unsaturated (UZ) and saturated zone (SZ). All components run simultaneously and exchange water between the different compartments during the simulation, with a maximum time step of 1 h for the OL and UZ compartments, 3 h for the SZ compartment and 5 s for the stream network compartment.

The horizontal resolution was set to 50 × 50 m and the vertical resolution varied from a couple of centimeters to several meters, depending on depth, soil type and saturation. The model consists of 10 computational layers (CLs), in general following the stratigraphy of the soil (Fig. 1C). Three of the CLs are located in the bedrock and seven in the soil. Due to the nature of the numerical implementation of ET and UZ processes in MIKE SHE, the uppermost CL needs to have a thickness sufficient to capture the influence of ET dynamics and the capillary rise of groundwater. In this model application, the thickness was set to 2.5 m, resulting in an averaging of the shallowest part of the soil stratigraphy into one CL in the model. To account for the observed high hydraulic conductivity in the upper 0.5 m of the till (Amvrosiadi et al., 2017; Bishop et al., 2011; Ågren et al., 2014), a drainage function was activated in the model using the same method as implemented by Bosson et al. (2008).

Meteorological data drive the MIKE SHE model, as they provide the upper boundary condition. These data comprise locally-observed time-varying air temperature (T), P and PET (Table 3);

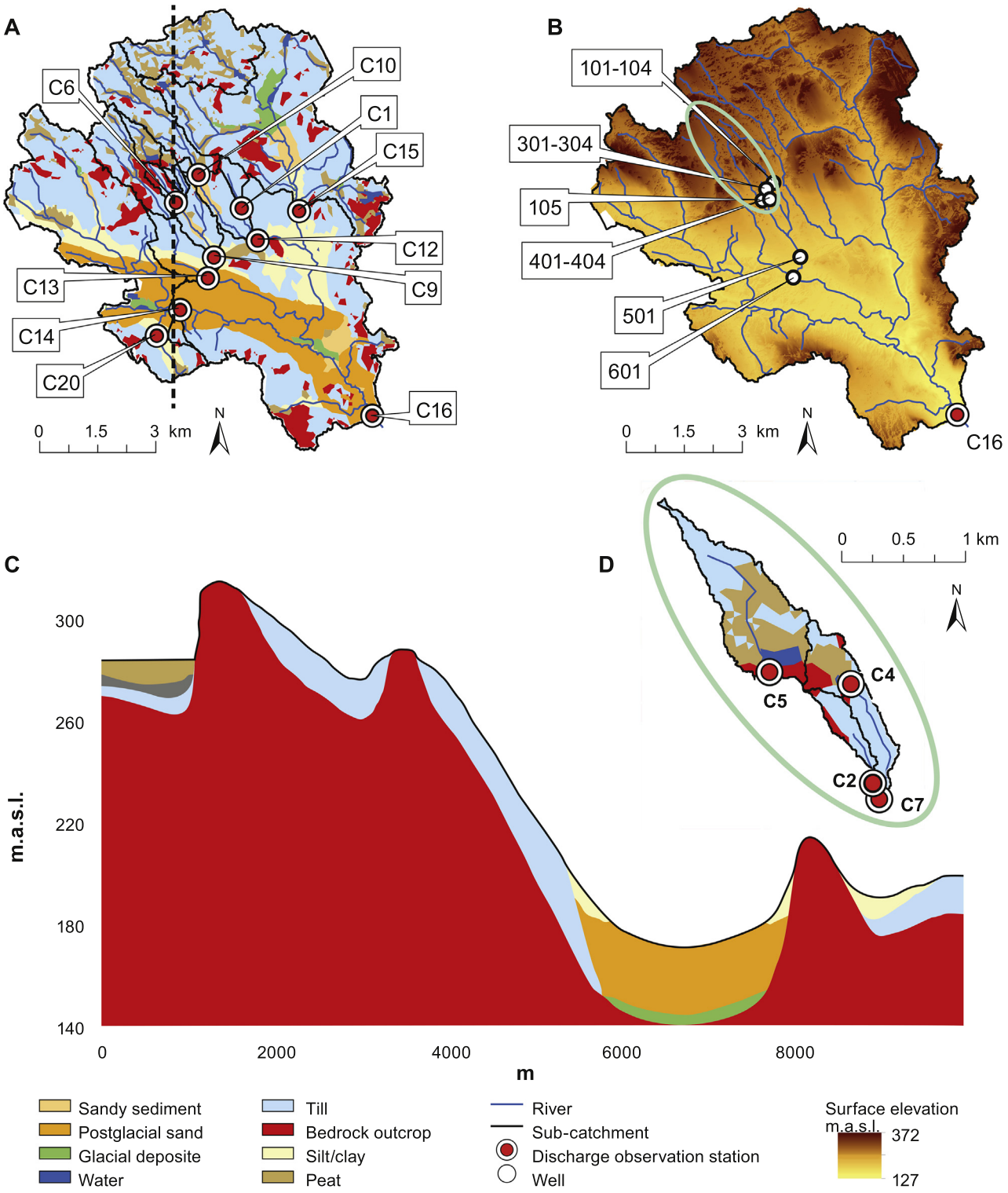

Fig. 1. Krycklan Catchment. **A**: Soil layer map including location of discharge observation stations and panel C (vertical black line). **B**: The Krycklan catchment, elevation (m.a.sl.) and location, rivers and groundwater wells. Area marked with green oval is shown in more detail in panel D. **C**: Conceptual model and soil deposits (north to south). **D**: Location of gauging stations C2, C4, C5 and C7.

P was corrected for wind and adhesion losses following Alexandersson (2003).

A no-flow bottom boundary condition was applied at 100 m depth. We assumed that surface and groundwater divides coincide, applying no-flow boundary conditions on the lateral boundaries, except for the areas with postglacial sand in the low topography areas of the catchment (Fig. 1A and B). A fixed head was used in the western and eastern parts of the postglacial deposits at the catchment boundaries. The fixed-head boundary corresponded to the water level of nearby lakes at the western boundary, and a mean value of groundwater head measurements at site C16 at the southeast boundary (Fig. 1A). Cycling one hydrological year until quasi-steady-state conditions were reached defined the initial conditions for the model.

Table 1
A: Sub-catchment gauging set up and main characteristics. **B**: List of groundwater wells*. The table also shows the depth, soil type and measurement period. Fig. 1B shows the location of the wells.

A	Site characteristics and gauging set up						
Site	Gauge type	Area (km^2)	Elevation (m.a.s.l.)	Main catchment characteristics (%)			Description
				Forest	Mire	Lake	
C2	90° V-notch weir in heated house	0.12	273	99.9	0.0	0.0	Forest-dominated catchment
C4	90° V-notch weir in heated house	0.18	287	55.9	44.1	0.0	Major part dominated by peatland
C5	H-flume in heated house	0.65	292	54.0	39.5	6.4	Lake outlet, major part dominated by peatland
C7	90° V-notch weir in heated house	0.47	275	82.0	18.0	0.0	Forest-dominated catchment affected by peatlands
C16	Natural section (bridge)	67.9	239	87.2	8.7	1.0	Main catchment outlet

B	Groundwater wells					
Well	Depth	Soil	Obs. Period		Frequency	Comment
			Start	End		
101	3.8	Till	08/19-82	10/14-16	weekly values	
102	2.4	Till	08/19-82	10/14-16	monthly values	Same location as 103
103	4.7	Till	08/19-82	10/14-16	monthly values	Same location as 102
104	3.2	Till	08/19-82	10/14-16	monthly values	
105	3.1	Till	08/19-82	10/14-16	monthly values	
301	3.3	Till	06/01-12	11/13-14	12 measurements for each well spread out over the observation period	
302	1.7	Till	06/01-12	11/13-14	12 measurements for each well spread out over the observation period	
303	4.7	Till	06/01-12	11/13-14	12 measurements for each well spread out over the observation period	
304	10.2	Till	06/01-12	11/13-14	12 measurements for each well spread out over the observation period	
401	2.5	Till	06/01-12	11/13-14	10 measurements spread out over the observation period	
402	1.4	Till	06/01-12	11/13-14	12 measurements for each well spread out over the observation period	
403	3.2	Till	06/01-12	11/13-14	12 measurements for each well spread out over the observation period	
404	9.7	Till	06/01-12	11/13-14	12 measurements for each well spread out over the observation period	
501	3.5	Till	06/01-12	11/13-14	7 measurements spread out over the observation period	Below a layer of 3 m silt/clay
601	5.2	Sand	06/01-12	11/13-14	9 measurements spread out over the observation period	Sand (layer 2)

* Four of the sites have heated houses at the gauging stations, allowing all-year-round measurements; C2 and C4 have been heated since 2011, C5 since 2012 and C7 since 1981. See Karlsen et al. (2016b) and Laudon et al. (2013) for more information regarding catchment characteristics and gauging set up.

2.3. Modelling procedure and calibration

We calibrated the MIKE SHE model based on time series of daily stream discharge and groundwater head data (Table 1) for the period 2009-01-01 to 2012-12-31. Fourteen sub-catchments have continuously monitored stream discharge (Karlsen et al., 2016b). The five sub-catchments C2, C4, C5, C7 and C16 (Fig. 1) are among the most studied locations within the catchment and together cover a representative range of the Krycklan landscape heterogeneity (Laudon and Sponseller, 2017). These sub-catchments were therefore used for calibration of our model, while the remaining nine were used for model validation (Laudon et al., 2013; Fig. 1). Groundwater levels, used for calibration and validation in this study, have been manually measured at 15 groundwater wells using different intervals of measurement, ranging from weekly to annual (Fig. 1B, Table 1B).

Hereafter, *Base Case* (B.C.) refers to the MIKE SHE model described in Sections 2.1 and 2.2. Based on the methodology developed by Aneljung and Gustafsson (2007) and Bosson et al., (2008), the model was calibrated using four main steps. Each step resulted in an updated model version (Fig. 2). Although some of the sub-catchments were the main targets for parts of the calibration, the full-scale model was run through all steps. Thus, changes made in a calibration step were evaluated for specific sub-catchments, where the investigated process or characteristics were clearly propagated in the result, but were then applied to the whole model domain.

The errors in discharge and hydraulic groundwater head results can be quantified by various methods (Bosson et al., 2008; Henriksen and Sonnenborg, 2005), and the choice of error estimation method depends on the main purpose of the model. For this study, the water balance and general model performance were the main interests, which motivated the use of accumulated discharge error in all steps and the Nash-Sutcliffe model efficiency (NSE) as error estimation metrics for the discharge results in later steps (Appendix C). If NSE is below zero, the observed mean is a better predictor than the model itself and if NSE reaches its maximum value of one, the model gives a perfect fit to observations (Krause and Boyle, 2005; Henriksen and Sonnenborg, 2005). Therefore, the objective of the calibration was to achieve a NSE value above zero, and to minimize the accumulated discharge error to approximately ±15%, which we defined as satisfactory in relation to measurement uncertainties (Bosson et al., 2008).

Groundwater heads are usually described using mean error (ME) or mean absolute error (MAE) and the accepted ME and MAE depends on the groundwater head variation of the catchment. In the case of Krycklan, the groundwater head varied by approximately 1–2 m at each observation point. By using the accumulated discharge error target of 15%, the ME and MAE target for the groundwater head should be within 0.3 m. It is recommended by Henriksen and Sonnenborg (2005) that use should be made of the performance criterion β that expresses the over-/under-prediction in relation to the groundwater head difference in the full-scale model range (Appendix C). If the model has high fidelity, β should have a value less than 0.01. The following Section describes each step of the calibration procedure (Fig. 2), with the aim of achieving the defined calibration targets.

2.3.1. Step 1: water balance on catchment and annual scale

The first calibration target was to capture the overall water balance (WB) for the entire catchment. The stream discharge at the Krycklan outlet (C16, Fig. 1A) and previous studies on the long-term water balance were used as calibration data. The annual PET (Table 3) was higher than the estimated ET presented in Laudon et al. (2013), 500 mm compared to 300 mm. Earlier MIKE SHE studies showed that the PET, used as input data, was very similar to the simulated total ET (Bosson et al., 2008). Applying the original PET data would have resulted in too much water being lost by ET processes. The lack of data on vegetation-specific transpira-

Table 2
General soil stratigraphy and hydraulic conductivities for each type of soil.

Soil type at surface	Depth below ground (m)	Soil type (vertically)	Kh (m/s)	Kv (m/s)	*Source*[*]
Bedrock outcrops	To bedrock	Bedrock	1 × 10^9	1 × 10^−9	Generic
Peat	5	Peat	1 × 10^−6	1 × 10^−6	Generic
	7	Clay	1 × 10^−9	1 × 10^−9	Generic
	To bedrock	Fine till	1 × 10^−6	1 × 10^−7	Local
Till	0.5	Coarse till	2 × 10^−6	2 × 10^−7	Local
	2.5	Mid till	2 × 10^−6	2 × 10^−7	Local
	To bedrock	Fine till	1 × 10^−6	1 × 10^−7	Local
Clay under lakes	5	Clay	1 × 10^−9	1 × 10^−9	Generic
	To bedrock	Fine till	1 × 10^−6	1 × 10^−7	Local
Sandy sediments	0.8	Sand	3 × 10^−5	3 × 10^−5	Local
	3	Silt/clay	1 × 10^−8	1 × 10^−8	Generic
	To bedrock	Fine till	1 × 10^−6	1 × 10^−7	Local
Silt/Clay	3	Silt/clay	1 × 10^−8	1 × 10^−8	Generic
	To bedrock	Fine till	1 × 10^−6	1 × 10^−7	Local
Postglacial sand	1.2	Silt/sand	1 × 10^−7	1 × 10^−7	Local
	3.8	Sand	3 × 10^−5	3 × 10^−5	Local
	4	Silt/clay	1 × 10^−8	1 × 10^−8	Generic
	0.9 × max depth	Sand	3 × 10^−5	3 × 10^−5	Local
	To bedrock	Gravel	1 × 10^−4	1 × 10^−4	Generic
Glacial deposits	To bedrock	Gravel	1 × 10^−4	1 × 10^−4	Generic

[*] Calculations based on grain-size analyses from sampling taken during drilling of wells as well as measurements taken in the field constitute the locally-derived data. Generic data are literature values (Bosson et al., 2010; Knutsson and Morfeldt, 2002).

Table 3
Meteorological data, including precipitation (P), corrected precipitation according to (Alexandersson, 2003) (P corrected), potential evaporation (PET) and mean annual air temperature (MAAT). The last column in the table lists the mean values for the observed period 2007–2014.

Year	2007	2008	2009	2010	2011	2012	2013	2014	Mean
P (mm)	563	659	666	613	646	829	648	584	651
P corrected (mm)	598	700	706	652	681	878	686	618	690
PET (mm)	457	506	546	530	579	397	485	520	503
MAAT (°C)	3.2	2.1	1.5	1.5	3.3	2.2	3.7	6.0	2.9

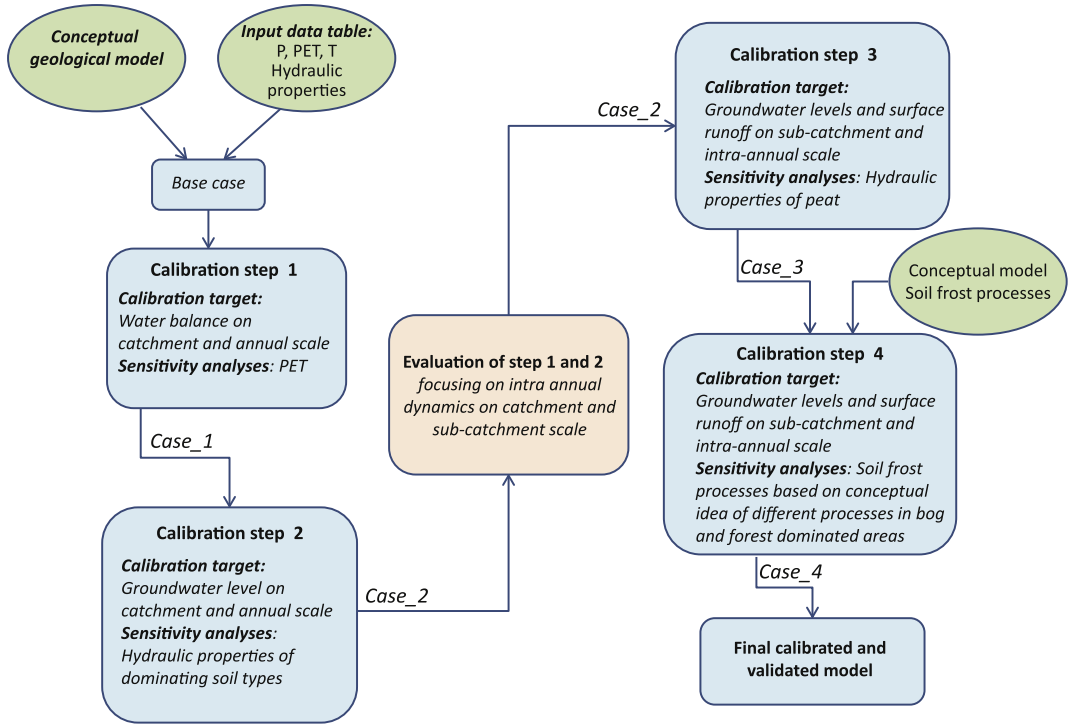

Fig. 2. Calibration steps. The stepwise calibration procedure based on (Bosson et al., 2010,2008). Every calibration step (1–4) ends with a new model setup, with a new name. For example, calibration set 1, results in a new modelling set up called Case_1, which is used in the next calibration step. In this way the model is stepwise improved until the final calibrated model is obtained.

tion parameters motivated our decision to base the sensitivity analyses on the calculated PET input data instead of analyzing the ET parameters used in MIKE SHE (Kristensen and Jensen, 1975). Therefore, the analysis was based on different magnitudes of reduced PET, with the main target being to minimize the accumulated discharge error.

2.3.2. Step 2: groundwater head on a catchment and annual scale

In the second calibration step (Fig. 2), a sensitivity analysis was made of the hydrological properties of the dominant soil types in the area, by increasing and decreasing their respective initial vertical/horizontal hydraulic conductivity by a maximum factor of ten (Appendix A, Table A1). The main target was to minimize accumulated discharge error and the groundwater head MAE and ME.

2.3.3. Evaluation of steps 1 and 2

After Steps 1 and 2, an evaluation was made to understand how the calibration at the full-catchment scale had affected the water balance at a sub-catchment scale. The evaluation focused on the representative sub-catchments C2, C4, C5, and C7 (Fig. 1D). Calculated and observed discharges were analyzed using the accumulated discharge error, the NSE values and a visual analysis of the concordance between the observed and simulated discharge time-series. The analysis was made to ensure that the changes made in Steps 1 and 2 were favorable also at the sub-catchment scale.

2.3.4. Step 3: groundwater head and surface runoff at a sub-catchment and intra-annual scale

In Step 3 (Fig. 2), the effects of hydraulic properties of the soils in the representative sub-catchments were further analyzed. Peat is a dominant soil type in both C4 and C5, and also affects C7. Only a few observations of peat have been made in Krycklan, including hydraulic properties, depth and vegetation of the mires at sites C4 and C5 (Laudon et al., 2013; Lidman et al., 2013). Observations indicate a high porosity of the peat, which results in high storage capacity in the peat-dominated sub-catchments. Therefore, in Step 3, an analysis of the influence of peat properties, including drainable pore space and hydraulic conductivity (Appendix A, Table A2), was performed. In this step, our focus was on increasing NSE for the discharge results, while also making a visual comparison of simulated and measured time-series.

2.3.5. Step 4: the influence of soil frost processes

Previous studies in Krycklan indicate that the hydrological pathways during spring flood differ between forest-dominated and mire-dominated catchments with higher event water ratios in the latter (Laudon et al., 2007; Peralta-Tapia et al., 2015). Based on this observation, a conceptual model was defined that specified the difference in the dominant hydrological processes related to soil freezing between mires and forest-dominated areas (Fig. 3).

Although there is no thermal component in MIKE SHE, there is a method for implementing soil frost processes, as presented by Bosson et al. (2010) and tested for permafrost areas by Johansson et al. (2015). In summary, three main processes were identified as important in describing the hydrology under frozen conditions: i) ice accumulation on the ground surface, ii) reduced infiltration capacity of frozen soil and iii) reduced transport capacity when soil is frozen. In this study, we focused on ii) and iii) since they are relevant for seasonally-frozen conditions during the winter and spring. These processes are described in the model by time-varying properties of infiltration capacity and hydraulic conductivity driven by soil and air temperature (Bosson et al., 2010). To analyze the range of effects from implementing such frost-process representation for peatland and forest-dominated areas, we developed six sub-cases (4a–f, Table 4) stemming from the conceptual model (Fig. 3). The purpose was to evaluate the impact of the level of frozen soil saturation on the infiltration and transport capacity during snowmelt.

Observations indicate saturated conditions and water on the ground surface at the peatlands (Peralta-Tapia et al., 2015). Due to data limitations, we therefore assumed that the thermal regime in the peatlands follows the same pattern as the lake ice in the catchment, i.e., the duration of frost in the peatlands was modelled using time-lapse photos of lake ice break-up and air-temperature data.

In the forested areas, the frost duration was governed by the observed soil temperature data, and we therefore assumed that the soil is affected by soil frost for temperatures below 0 °C at a depth of 10 cm. When data were missing at 10 cm depth, data from 5 cm depth were used. A reduced transport capacity was assumed during frozen soil conditions, and the extra transport capacity in the upper 0.5 m of the model was reduced to zero during this period. Our main target for this step was to obtain a low accumulation of discharge errors and to achieve high values of NSE for the stream discharge, while also minimizing MAE and ME for the groundwater heads.

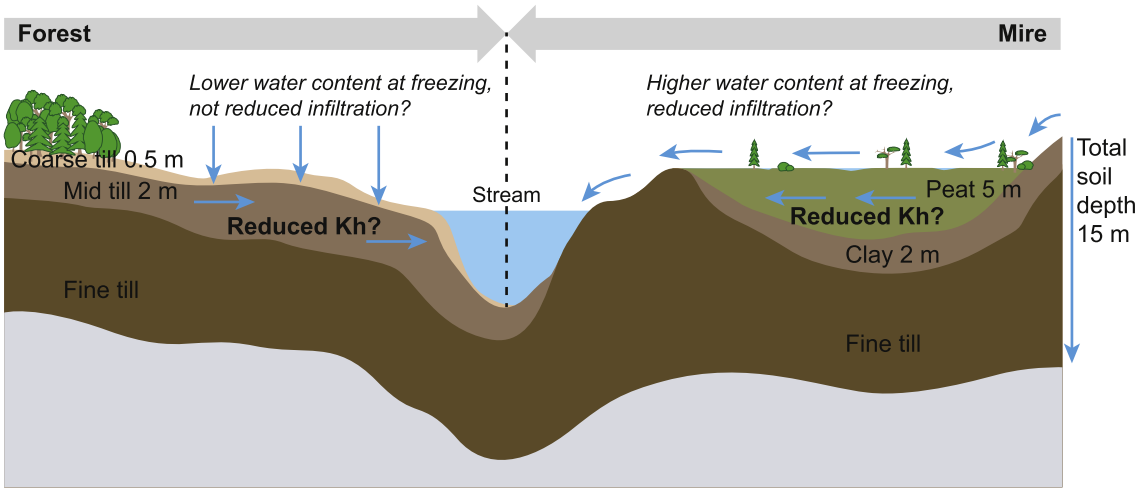

Fig. 3. Conseptual model: Soil frost. Conceptual model for the hydrological processes during soil frost conditions in a forest (left) and mire (right) dominated catchment. The two main frost processes that are evaluated is reduced flow in the upper part of the soil (reduced Kh) and/or reduced infiltration (Table 4).

Table 4
Sensitivity analysis of soil frost processes on peatlands and forested soils, evaluated in calibration Step 4 (Fig. 2), including reduced infiltration and reduced transport capacity in the upper part.

Sub-case	Reduced infiltration		Reduced transport capacity in upper 0.5 (m)	
	Peatland	Forest	Peatland	Forest
4a	X			
4b		X		
4c			X	
4d				X
4e	X		X	
4f		X		X

3. Results

3.1. Step 1: water balance on a catchment and annual scale

For the Base Case model, the simulated accumulated discharge was 44% lower than observed and approximately 80% of the P left the model as ET during the simulated years of 2009–2011, which was more than the long-term annual average of 50% reported from the catchment (Laudon et al., 2013). Reducing the PET had a positive effect both on matching the accumulated discharge at C16 as well as on the conforming more closely to the observed overall water balance (Tables 5 and 6A).

To reach a water balance in which approximately 50% of the P converts to ET on the full catchment scale, the PET had to be reduced to 40% of the original input data (Table 3). After this change of the PET (Step 1) the accumulated discharge error was reduced to 3% and the ratio between the actual evaporation and P was reduced to approximately 50% (Table 5). Note that during 2012, when an annual P of 880 mm was experienced, the evapo transpiration-precipitation ratio was lower than 50% after the reduction of the PET. The reduced PET was used in later calibration steps since it gave the optimal water balance result for C16.

3.2. Step 2: groundwater head on a catchment and annual scale

The groundwater calibration in Step 2 focused mainly on the hydraulic properties of the dominant soil types in the area: till, silt/clay and sand. A reduction of the hydrological conductivities in the upper parts of the till had a positive effect on prediction of the groundwater heads and dynamics around site C7 (Fig. 4A and B) and on the ME and MAE values (Table 6B). An increase of the horizontal conductivity in the sand and the vertical conductivity in the silt/clay resulted in the groundwater heads reaching the observed values in wells 501 and 601 (Fig. 4C and D). The changes also gave a positive effect at C16 concerning peak stream discharge during intense rain, e.g., autumn of 2012 (Fig. 4E).

3.3. Evaluation of step 1 and 2

The model efficiency values (NSE) increased for all sub-catchments, when comparing results from Step 1 and Step 2 (Table 6). However, C4 still had a value below zero, which indicates that the model is not accurately representing this sub-catchment. These calibration steps, Step 1 and Step 2, affected C2 and C7 the most. For example, the C2 accumulated discharge error reduced from 28% to 6% (Table 6A) and the impact of rain events on peak stream discharges was also reduced, e.g., during the autumn of 2012 (Fig. 5A). In that sense, calibration Step 2 improved the results of Step 1. In contrast, sites C4 and C5 exhibited smaller changes than for C2 and C7, both in peak stream discharges during rain events and accumulated discharge (Table 6A and Fig. 5A–D). In summary, we could see the largest differences between Step 1 and Step 2 in the forest-dominated sub-catchments.

3.4. Step 3: groundwater head and surface runoff at a sub-catchment and intra-annual scale

In Step 3, a higher porosity and storage capacity of peat was introduced in the model. This had a positive effect on the modelling results obtained for sites C4 and C5 by reducing the peak discharges during rain events (Fig. 6A–B), and generally increasing the model efficiency for all sites, except for site C5 (Table 6A). However, a high porosity and storage capacity of the peat also reduced the amount of water reaching the streams during snowmelt, which increased the accumulated discharge error in spring (Fig. 7C and Appendix B, Table B1). A high porosity and storage capacity of the peat also provided the streams at site C4 and C5 with more water as groundwater flow than upstream flow during snowmelt, as compared with Case 2 (Fig. 7D). In summary, a high porosity and storage capacity of the peat improved the results during rain events, but worsened the results during spring, especially for C5 which had the largest accumulated flow reduction, from an error of −21% to −41% (Appendix B, Table B1).

3.5. Step 4: the influence of soil frost processes

Reducing the infiltration rate during winter for the peatlands resulted in a higher proportion of water arriving as overland flow to the stream during snowmelt (Fig. 7D and E). By also applying a decreased transport capacity of the soil, even less water infiltrated during snowmelt and in total more water arrived to the peatland streams, which is in line with empirical observations (Laudon et al., 2007).

Compared with peatlands, introduction of soil frost processes in the model did not improve the result for areas dominated by forest. For example, a reduction of the transport capacity of the soil resulted in a delayed effect of the snowmelt (7A). Some of the groundwater wells also exhibited an increased groundwater head during the winter periods (Fig. 7B), which has not been observed in the area.

Table 5
Precipitation (P) and calculated evapotranspiration (ET) (mm) for each simulated year using the original PET input data (PET 100%) and PET input data reduced to 40% of the original (PET40%). The table also includes the P and ET difference (P-ET) as well as the ET to P ratio (ET/P).

	Water balance results ET_40%								
Year	2009		2010		2011		2012		Obs. average
	PET 100%	PET 40%	PET 100%	PET 40%	PET 100%	PET 40%	PET 100%	PET 40%	
Total P (mm)	706	706	652	652	681	681	880	880	614
Total ET (mm)	533	338	523	330	554	358	408	251	303
P-ET (mm)	173	368	129	327	129	325	473	628	311
ET/P ratio (%)	75	48	80	50	81	52	46	29	50

Table 6
A: Discharge performance measures for the Base Case (B.C.) and Case 1–4(e) (c. 1 – c.4) (2009–2012), as well as validation of Case 4e (validation) (2009–2014). The Table includes accumulated discharge error (Acc. error (%)) and the NSE values for the calibrated discharge stations C2, C4, C5, C7 and C16 as well as for the other observation stations in Krycklan used for validation. **B**: Groundwater head performance measures for the Base Case (B.C.) and Case 1–4(e) (c. 1 – c.4), as well as validation of Case 4e (validation) (2009–2014). The Table includes MAE and ME for all Cases.

A	Discharge results											
	Acc. error (%)						NSE					
	B.C.	c. 1	c. 2	c. 3	c. 4	validation	B.C.	c. 1	c. 2	c. 3	c. 4	validation
C2	−40	28	6	5	5	3	0.6	0.4	0.7	0.7	0.7	0.7
C4	−37	11	7	1	3	6	0.1	−0.7	−0.3	0.6	0.4	0.3
C5	−58	−18	−19	−29	−26	−23	0.3	0.7	0.7	0.6	0.8	0.8
C7	−34	19	18	18	18	20	0.6	0.2	0.6	0.8	0.7	0.7
C16	−44	3	−2	−4	−3	−3	0.4	0.2	0.6	0.8	0.7	0.7
C1	−44	16	17	17	16	14	0.6	0.6	0.8	0.8	0.8	0.7
C6	−47	−4	−5	−11	−9	−7	0.4	0.6	0.8	0.8	0.8	0.8
C9	−46	4	0	−2	−2	−3	0.5	0.7	0.8	0.8	0.8	0.8
C10	−46	−3	−4	−6	−5	−5	0.5	0.2	0.6	0.7	0.8	0.7
C12	−44	17	15	12	11	9	0.5	0.5	0.7	0.8	0.8	0.8
C13	−41	15	3	0	−1	1	0.4	0.3	0.7	0.7	0.8	0.8
C14	−29	26	25	26	26	32	0.0	−0.9	0.2	0.4	0.3	0.3
C15	−54	−12	−16	−18	−18	−13	0.4	0.4	0.6	0.7	0.7	0.7
C20	−56	−17	−21	−20	−21	−17	0.0	−0.4	0.0	0.2	0.2	0.1

B	Groundwater head results					
	ME/MAE					
	B.C.	c. 1	c. 2	c. 3	c. 4	validation
101	−0.8/0.8	0.3/0.5	−0.4/0.4	−0.2/0.4	−0.2/0.4	−0.2/0.4
102	−0.7/0.7	0.0/0.3	−0.3/0.4	−0.3/0.3	−0.3/0.3	−0.3/0.3
103	−0.4/0.5	0.4/0.5	−0.1/0.2	−0.2/0.3	−0.2/0.3	−0.2/0.3
104	−0.4/0.4	0.1/0.2	0.3/0.3	0.3/0.3	0.3/0.3	0.3/0.3
105	−0.4/0.4	0.1/0.4	0.1/0.3	0.1/0.3	0.1/0.3	0.1/0.3
301	−0.1/0.1	0.0/0.1	0.0/0.1	0.0/0.1	0.0/0.1	−0.1/0.2
302	−0.2/0.2	−0.1/0.2	−0.2/0.2	−0.2/0.2	−0.2/0.2	−0.1/0.2
303	−0.1/0.2	−0.1/0.2	−0.1/0.2	−0.1/0.2	0.0/0.2	−0.1/0.2
304	0.1/0.1	0.2/0.2	0.2/0.2	0.2/0.2	−0.1/0.2	0.1/0.3
401	−0.3/0.3	−0.3/0.3	0.0/0.1	0.0/0.0	0.0/0.1	0.2/0.2
402	0.1/0.1	0.2/0.2	0.6/0.6	0.6/0.6	0.6/0.6	0.7/0.7
403	−0.3/0.3	−0.2/0.2	0.1/0.1	0.1/0.1	0.1/0.1	0.4/0.4
404	1.4/1.4	1.3/1.3	1.0/1.0	1.0/1.0	1.0/1.0	0.8/0.8
501	−2.3/2.3	−1.6/1.6	−0.3/0.3	0.2/0.2	0.2/0.2	0.2/0.3
601	−2.1/2.1	−1.3/1.3	−0.3/0.3	−0.4/0.4	−0.4/0.4	−0.2/0.2

Case 4e had the most promising results, increasing the amount of water that the streams received while keeping the NSE values for the discharge high and maintaining the ME and MAE for the groundwater flow at most sites (Table 6B). The effect is mostly visible during the spring period, when, e.g., C5 showed a reduction in its accumulated discharge error from −41% to −25% (Appendix B, Table B1).

3.6. Validation and final calibrated values

The final model, Case 4e, has a high porosity and storage capacity of the peat, with peat that freezes during the winter months. It includes a reduction in the extra horizontal flow in the upper part of the peat, as well as introducing an impermeable soil frost layer. This model case was most successful at both reproducing accumulated discharge at the streams outlets of the sub-catchments (Fig. 8), as well as reproducing the groundwater fluctuations and peak discharges during the calibration period (Table 7).

We tested the performance of the model using the validation period of 2013–2014, as well as the remaining nine sub-catchments (Fig. 8 and Table 6). Generally, the NSE value improved between Cases 2 and 3, Also, the accumulated error improved between Case 3 and 4, while keeping the NSE values above zero and still higher than in Case 2 (Table 6).

The average accumulated discharge error for the calibration catchments C2, C4, C5, C7 and C16 combined was 0.7% for the total model period (2009–2014), with the largest accumulated errors arising from C5 and C7 (Table 6A), which both had a final error above the target of 15%. Looking at all gauged sites in Krycklan, however, 80% of the catchments had an accumulated discharge error of lower than 15%, all with final NSE values above zero and with an average NSE value of 0.6. Furthermore, the model (Appendix B, Fig. B1) has also captured specific discharge patterns for the sub-catchments.

The average MAE values for the groundwater head results were approximately 0.3 m for the total model period (2009–2014), and in total 70% of the simulated wells had a MAE lower (or equal) to the ±0.3 m target. For the simulated years, the maximum observed groundwater head, 257 m.a.s.l., occurred at well 101 and the lowest observed groundwater head, 170 m.a.s.l, occurred at well 601, giving an overall difference in groundwater head (Δh_{max}) of 87 m. This, together with the average ME for the total simulated period at 0.12 m, gave a β value of 0.0014, which is below the 0.01 target, meaning that the simulated values have high fidelity (Table 6b, Appendix C).

4. Discussion

Our final model of the Krycklan catchment was successful in recreating observed accumulated discharge and groundwater patterns on both an inter- and intra-annual scale. This study demonstrates the importance of considering processes and characteristics on a sub-catchment scale; furthermore, the results illustrate that catchments are complex systems with different hydrological processes interacting in both time and space.

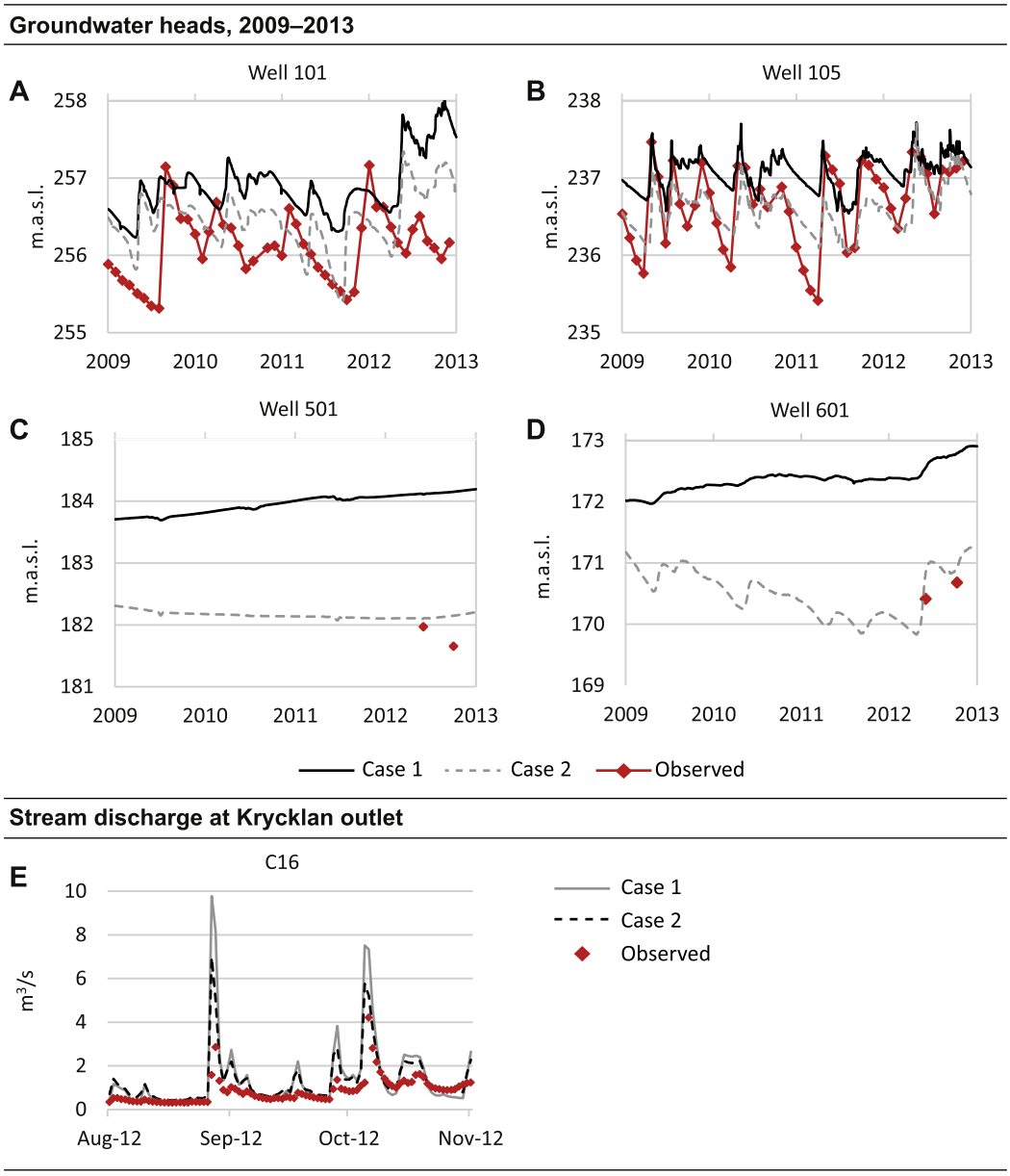

Fig. 4. Result step 2. **A–D**: Groundwater heads (m.a.s.l.) for case 1 and case 2, compared to observed for well 101 (A), well 105 (B), well 501 (C) and well 601 (D). **E**: Stream discharge at site C16 during the autumn of 2012.

4.1. Overland water and groundwater partitioning

Generally, our model was successful in simulating groundwater and streamflow observations for all years. For example, site C2 received less specific discharge than C4 and C5, which is in accordance with the empirical data. Large variability in specific discharge between the Krycklan sub-catchments has previously also been observed by (Karlsen et al., 2016a,b) based on 5 years of monitoring data. In that case, the annual differences in specific discharge among catchments were linked to the spatial variation of snow accumulation and ET.

In this study, the variations in specific discharges were explained by the surface and groundwater interactions on an annual and intra-annual time scale using a numerical integrated model. Although the P and ET are similar between the sub-catchments (Appendix B, Fig. B2 & Table B3), the modelled specific discharge varied. According to model results (Appendix B, Fig. B3), the water that is not lost by ET or exported as local river discharge, mainly contributes to changes in groundwater storage and to groundwater flow exiting the sub-catchments. The water that leaves its corresponding sub-catchment as groundwater flow without adding water to the rivers, i.e., through deeper flow paths, explains the variability in recharge to the streams. Differences in sub-catchment characteristics, such as soil properties and freeze-thaw processes, can explain this groundwater flow variability.

4.2. Model discrepancies

The main deviations between observed and calibrated specific discharge are most clearly visible when comparing 2011 and 2013 (Appendix B, Table B2). The year 2011 had low P and high ET, compared with the annual average values, resulting in low runoff to the rivers. In contrast, 2012 had high precipitation and low ET resulting in more runoff to the rivers than average. Although 2013 had precipitation and ET values close to the long-term annual average (Laudon et al., 2013), the simulated river runoff was higher

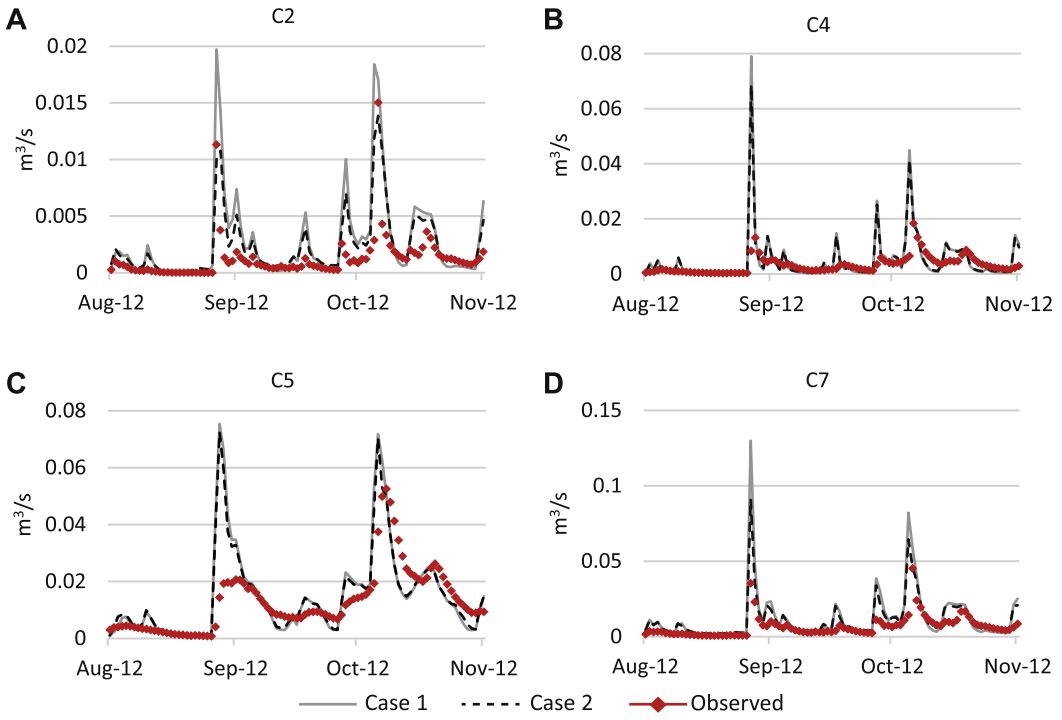

Fig. 5. Result step 2: Sub-catchments. **A–D**: Stream discharge at C2 (A), C4 (B), C5 (C) and C7 (D) for autumn 2012 for Case 1 and Case 2.

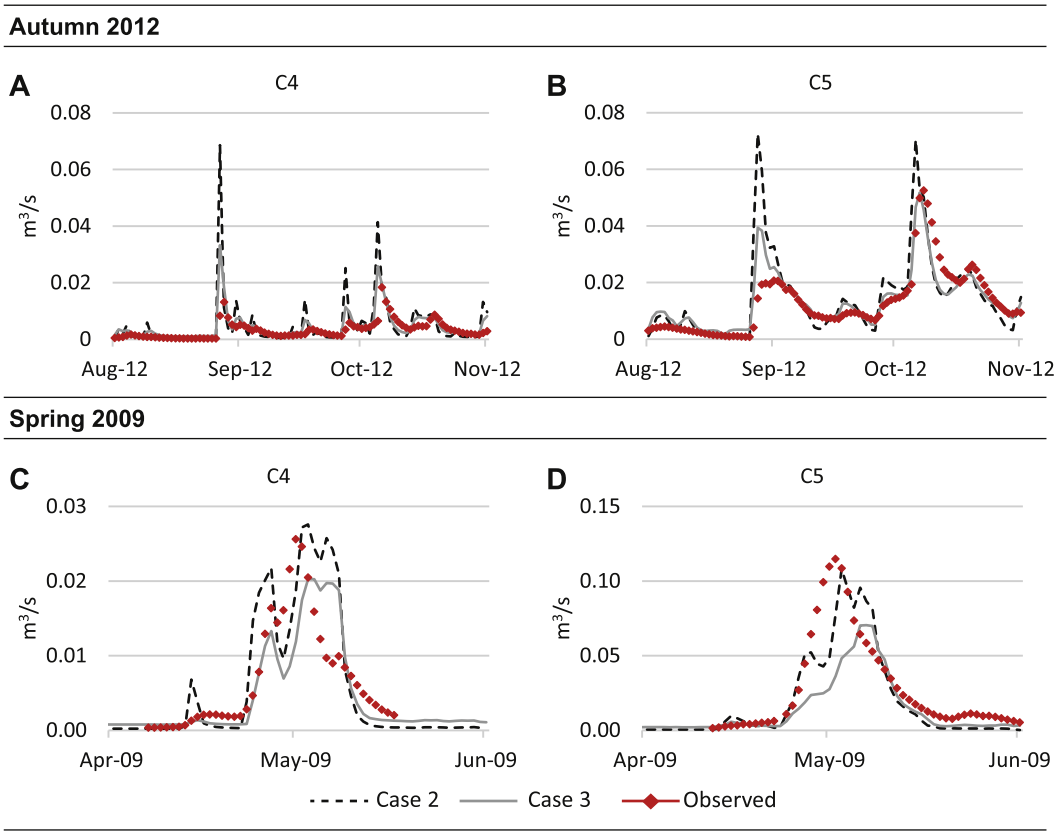

Fig. 6. Result step 3. **A–D**: Stream discharge at site C4 (A) and C5 (B) for autumn 2012 and stream discharge at site C4 (C) and C5 (D) for spring of 2009.

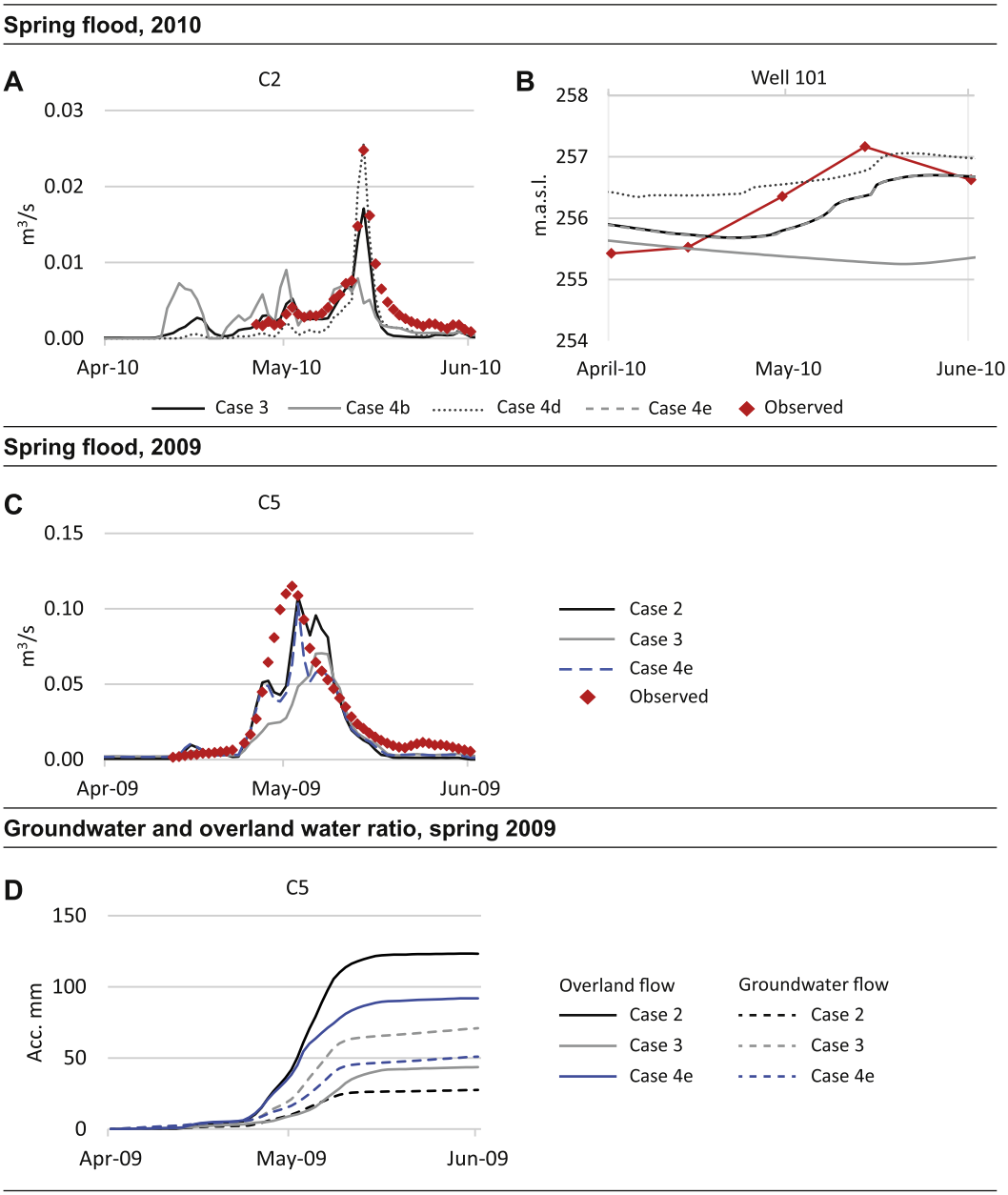

Fig. 7. Result step 4. **A–B**: Stream discharge results for site C2 (A) and groundwater heads for well 101 (B) during spring 2010. The results includes; Case 3 (high porosity and storage capacity of the peat), Case 4b (reduced infiltration during the winter in the forest), Case 4d (reduced horizontal flow during the winter in the forest) and case 4e (reduced infiltration and horizontal flow during the winters at the peatlands). **C–D**: Stream discharge results for C5 (C) and groundwater overland water ratio at C5 during spring 2009. The results includes; Case 2 (reduced ET), Case 3 (high porosity and storage capacity of the peat) and case 4e (reduced infiltration and horizontal flow during the winters at the peatlands).

than observed. The explanation for this is the variability in storage, where excess water from the wet 2012 remained in the catchment during 2013, resulting in increased modelled runoff even at the sub-catchment scale (Appendix B, Fig. B1).

Although there were deviations between simulated results and observations, the main pattern of specific discharge differences between sub-catchments was well captured (Appendix B, Fig. B1). What was important in achieving this result was our recognition of the role of heterogeneous landscape processes, including variability in soil frost. To explain the remaining deviations between simulated results and observations we need to further investigate sub-catchment processes and characteristics, so that model discrepancies can be reduced in future studies. The remaining deviations may be due to lack of specific information regarding ET differences between sub-catchments and this is yet to be included in the model. Deviations may also occur due to sub-catchment characteristics and processes not yet included in the model, such as lake ice, mainly affecting C5 and C15, and the detailed composition of the glacial deposits mainly affecting C14.

4.3. The importance of soil characteristics and soil frost

Peat is the most influential soil type with regard to its effect on peak stream flows during rain events (Fig. 6). However, the importance of this soil type was overlooked in Step 1 and Step 2 due to the full-scale calibration approach adopted, which supports the relevance of undertaking sub-catchment-scale investigations. A higher porosity and storage capacity of the peat reduces the impact

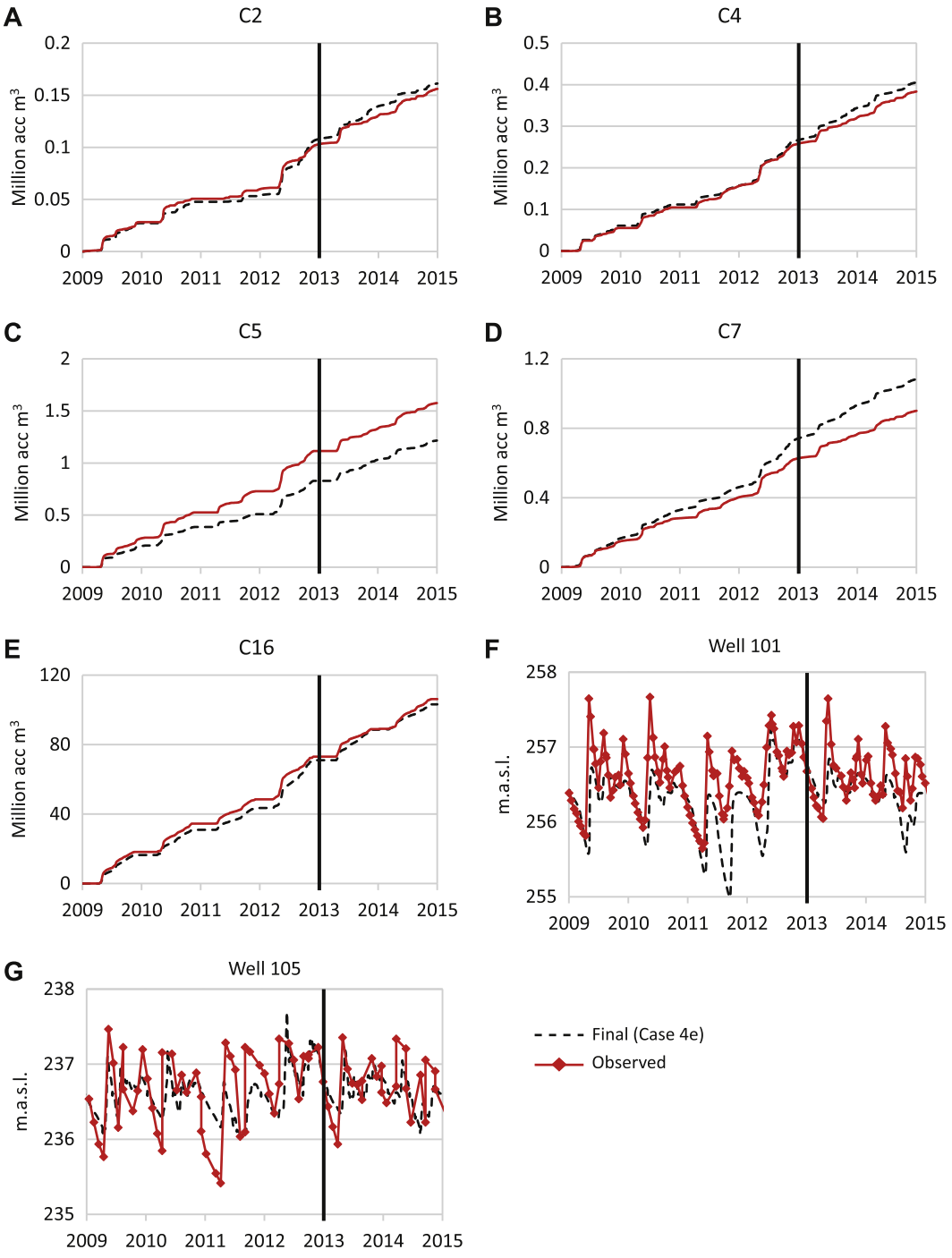

Fig. 8. Accumulated discharge result. **A–G**: Accumulated discharge result for site C2 (A), C4 (B), C5 (C), C7 (D) and C16 (E). Results include both observed accumulated discharge and the final modelled (case 4e) accumulated discharge results for calibration (2009–2012) and validation period (2013–2014). The black vertical line marks the end of the calibration period and start of the validation period at 2013-01-01.

of peak flows and allows for more infiltration in the area. By the introduction of soil frost in the peatland areas, more of the water arrived as overland flow, increasing the volume of water to the streams (Fig. 7). Introduction of peat with higher porosity and storage capacity, as well soil frost, improved the results.

In contrast to peatlands, neither a reduced infiltration capacity nor a reduced transport capacity improved the result in forest-dominated areas. By reducing the infiltration capacity of the soil, in Case 4b, more water arrived as overland flow to the streams, which is in agreement with observations at the groundwater wells and the gauging stations for the forested sub-catchments (Fig. 7A and B). Reducing the horizontal flow during winter, in Case 4d, delayed the water reaching the streams, resulting in a delayed discharge response and smaller fluctuations in groundwater head than were observed (Fig. 7A and B). This indicates that soil frost does not significantly influence the groundwater flow in forested areas. The low water content at freezing therefore allows snowmelt water to infiltrate the soil despite frozen conditions, which is in line with observations (Nyberg et al., 2001; Laudon, 2004; Peralta-Tapia et al., 2015).

Table 7
Initial and final calibrated parameters (Case 4e), including horizontal (Kh) and vertical (Kv) parameters for the soil, the peat characteristics (drainable porosity and unsaturated zone characteristics) and the increased Kh in the upper 0.5 m of the soils in Krycklan (m/s).

		Saturated zone			
		Initial values		Calibrated values	
	Unit	Kh	Kv	Kh	Kv
Till (depth 0.5 m)	m/s	2 × 10^−6	2 × 10^−7	2 × 10^−5	2 × 10^−6
Till (depth 2.5 m)	m/s	2 × 10^−6	2 × 10^−7	2 × 10^−5	2 × 10^−6
Silt/clay	m/s	1 × 10^−8	1 × 10^−8	1 × 10^−8	1 × 10^−7
Sand	m/s	3 × 10^−5	3 × 10^−5	3 × 10^−4	3 × 10^−5
Peat	m/s	1 × 10^−6	1 × 10^−6	1 × 10^−4	5 × 10^−5
		Drainable porosity			
		Initial values		Calibrated values	
Peat	%	10		80	
		Unsaturated zone			
		Initial values KS		Calibrated values KS	
Peat	m/s	1 × 10^−6		1 × 10^−4	
		Increased Kh in the upper 0.5 of the soil (m/s)			
		Initial values		Calibrated values	
Till	m/s	4 × 10^−7		4 × 10^−7	
Peat	m/s	Increased Kh not applied		1 × 10^−6	
Silt/clay	m/s	Increased Kh not applied		1 × 10^−6	

Studies made in continuous and discontinuous permafrost environments have suggested that soil frost reduces infiltration and increases surface runoff during snowmelt (Hayashi et al., 2004; McNamara et al., 1997; Metcalfe and Buttle, 2001). Furthermore, at Krycklan, studies including stream water tracer analyses have indicated that soil frost is a significantly important factor for surface and groundwater partitioning, especially in peatland areas (Buffam et al., 2007; Laudon et al., 2007). For example, Laudon et al. (2007) concluded that the composition of surface water and groundwater in streams during spring flood varies depending on landscape characteristics in the sub-catchments of the studied area. By using a stable isotope analysis of stream water, the study suggested that at C2, where till is the main soil type, the spring stream water is dominated by groundwater, whereas at C4, which is peatland dominated, the spring flood is dominated by overland flow. We argue that, due to a higher saturation level when peatlands freeze, the soil becomes less permeable and in some situations impermeable compared with soils with a lower saturation level (Peralta-Tapia et al., 2015). By introducing soil frost processes in the model and analyzing the effects on surface and groundwater partitioning, our study supports the findings of Laudon et al. (2007), who suggested that catchment characteristics and soil frost processes are important factors concerning surface and groundwater partitioning.

4.4. Evapotranspiration characteristics

PET had the largest influence on the overall water balance. By stepwise decreasing the PET, more water is partitioned as runoff, which allowed results to be obtained that were comparable with the observed data. However, there are uncertainties concerning the PET. These uncertainties originate from the method used to calculate the PET, and how the PET is implemented in the model. For the whole catchment we used a spatially uniform, but time-varying, PET, due to scarce information on the spatial distribution of the ET. Although the model takes differences in the catchment characteristics into account, the model-calculated ET remained approximately the same between sub-catchments (Appendix B, Table B3). Some differences between sub-catchments can, however, be seen when comparing ET contributions, mainly when comparing interception and surface-water-evaporation contributions.

In summary, ET may have a significant role in creating the model-calculated differences in specific discharge between sub-catchments, since there are some discrepancies between the model and observations. In a previous study of the Krycklan catchment, ET was identified as one of the main processes that explained the observed differences in specific discharge between sub-catchments (Karlsen et al., 2016a,b). However, since the model in the present study could capture the overall pattern of differences in specific discharges, despite the total ET being approximately equal between different sub-catchments, groundwater storage change and deep groundwater flow path may also have significant roles (as discussed in Section 4.1).

5. Conclusions

In this study, we have highlighted the role of sub-catchment heterogeneity. We found that local variations, in hydraulic properties and seasonal processes, are important at both a sub-catchment and a full catchment-scale. Although there are deviations between simulated results and observations, our current MIKE SHE model was able to capture the observed differences in groundwater-level fluctuations and specific discharge patterns within the Krycklan catchment.

Because the simulated ET was similar between sub-catchments, the main factor determining the specific discharge of a sub-catchment is its groundwater processes influenced by the hydraulic properties of the soils and soil frost processes. We have also shown that these characteristics have important influences on the partitioning of surface water and groundwater, which is a key consideration in the further study of biogeochemical cycling in this catchment. To capture the different small-scale processes, this study has emphasized the importance of defining representative sub-catchments within a full-scale catchment.

Acknowledgments

Several people have helped in different ways with this work, and we would like to thank everybody for their contributions. Specifically, we would like to thank Anders Lindblom, SKB, for creative help in the drawing of Figure 3 and the final preparation of all figures, and to the crew of the Krycklan Catchment Study (KCS) funded by SITES (VR), for advice and data collection. Special thanks also to Jan-Olof Selroos, SKB, for comments and advice on this article and Mike C. Thorne for a thorough language check and John Livsey for addition language revision. We would also like to acknowledge Svensk Kärnbränslehantering AB (SKB) for funding and the Danish Hydraulic Institute (DHI) for software access and expert consultation, without which this article would not have been possible.

Appendix A. – Initial values and calibration limits

The initial values and calibration targets for the main soil and peat characteristics used in this study are shown in Tables A1 and A2, respectively. These include the horizontal and vertical hydraulic conductivity as well as the increased hydraulic conductivity used to reduce the effect of averaging of the first CL.

Appendix B. – Results

The appendix comprises figures and tables showing results from simulation Cases 1–4. Figs. B1 and B2 and Tables B1–B3 includes ET, stream discharge and groundwater flow results, for C16 and the sub-catchments, C2, C4, C5 and C7. Fig. B1 and Table B1 include results from all monitoring stations in the catchment. Groundwater flow results for C2, C4, C5, C7 and C16 can be seen in Fig. B3.

Appendix C. – Performance criteria

The performance criteria and error-estimation parameters that have been evaluated for the model are shown below (Eq. B1–B5), where q_{obs_t} and q_{sim_t} are observed and simulated values respectively, t is time and Δh is the observed groundwater-head difference. See more about performance criteria in (Henriksen and Sonnenborg, 2005).

- Eq. C1 Accumulated discharge error

$$Accumulateddischargeerror = \left(1 - \frac{Accumulatedsimulateddischarge}{Accumulatedobserveddischarge}\right) \times -1$$

- Accumulated discharge error <0 The simulated discharge is less than observed
- Accumulated discharge error >0 The simulated discharge is more than observed

An estimation of the water balance error for a specific area compared with observations. The closer the error is to zero, the better the model is to represent the water balance. Simulated accumulated discharge is only added when there are observations for a given time. This is done to avoid the accumulated model discharge appearing to be larger than the observed discharge due to gaps in the observed data.

- Eq. C2 Mean error (ME)

$$ME = \frac{1}{n}\sum_{t}(q_{obs_t} - q_{sim_t})$$

Table A1
Calibration parameter initial values for the soil types till, silt/clay and sand, together with upper and lower calibration limits for Kh (horizontal hydraulic conductivity) and Kv (vertical hydraulic conductivity). The initial parameter values and parameter limits are used throughout the model.

	Soil hydraulic characteristics					
	Horizontal conductivity Kh (m/s)			Vertical conductivity Kv (m/s)		
	Initial	Lower	Upper	Initial	Lower	Upper
Silt/Clay	1 × 10^−8	1 × 10^−9	1 × 10^−7	1 × 10^−8	1 × 10^−9	1 × 10^−7
Coarse till	2 × 10^−6	2 × 10^−5	2 × 10^−7	2 × 10^−7	2 × 10^−8	2 × 10^−6
Mid till	2 × 10^−6	2 × 10^−5	2 × 10^−7	2 × 10^−7	2 × 10^−8	2 × 10^−6
Fine till	1 × 10^−6	1 × 10^−5	1 × 10^−7	1 × 10^−7	1 × 10^−8	1 × 10^−6
Sand	3 × 10^−5	3 × 10^−6	3 × 10^−4	3 × 10^−5	3 × 10^−6	3 × 10^−4
	Increased Kh in the upper 0.5 of the soil (m/s)					
	Initial		Lower		Upper	
Silt/Clay	0		1 × 10^−8		1 × 10^−6	
Till	4 × 10^−7		4 × 10^−8		4 × 10^−6	

Table A2
Calibration parameters initial values for peat, together with upper and lower calibration limits.

	Drainable pore space	Saturated hydraulic conductivity (m/s) (Ks)	Horizontal conductivity (m/s) (Kh)	Vertical conductivity (m/s) (Kh)
Initial	0.1	1 × 10^−6	1 × 10^−6	1 × 10^−6
Upper	0.8	1 × 10^−4	1 × 10^−4	1 × 10^−4
Lower	0.1	1 × 10^−6	1 × 10^−6	1 × 10^−6
	Increased Kh in the upper 0.5 of the soil (m/s)			
Initial	0			
Upper	1 × 10^−6			
Lower	1 × 10^−7			

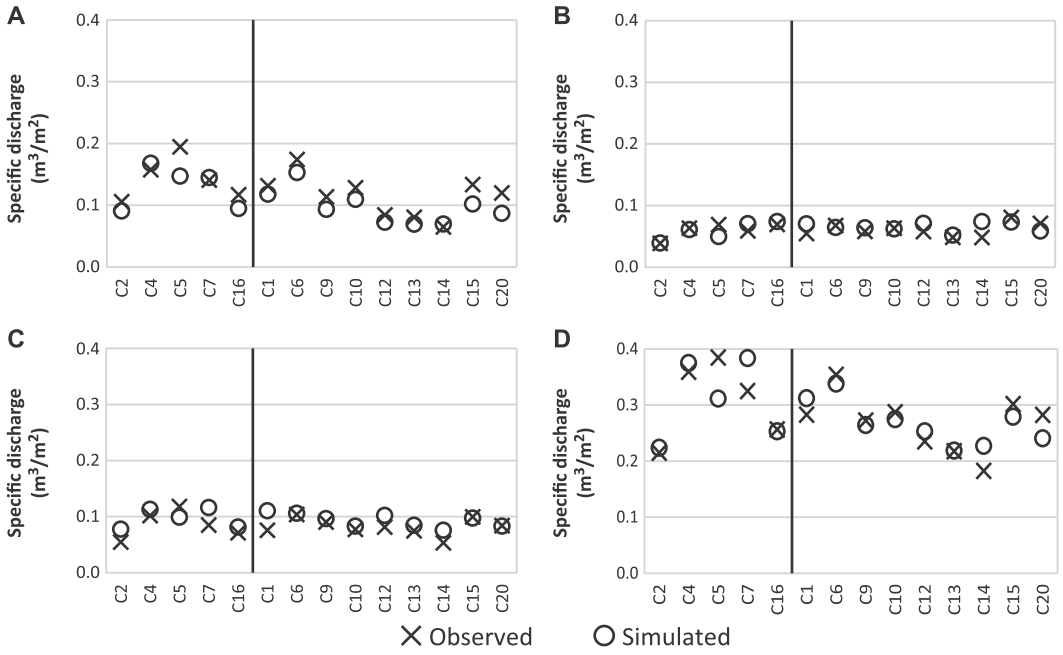

Fig. B1. Average specific discharge: Sub-catchments. Average specific discharge for each sub-catchment, observed and simulated (2009–2014). Shown to the left and right of the black vertical line, are the calibrated and validated discharge stations respectively. **A**: spring average (mar-apr), **B**: summer average (jun-aug), **C**: autumn average (sept-nov) **D**: yearly average.

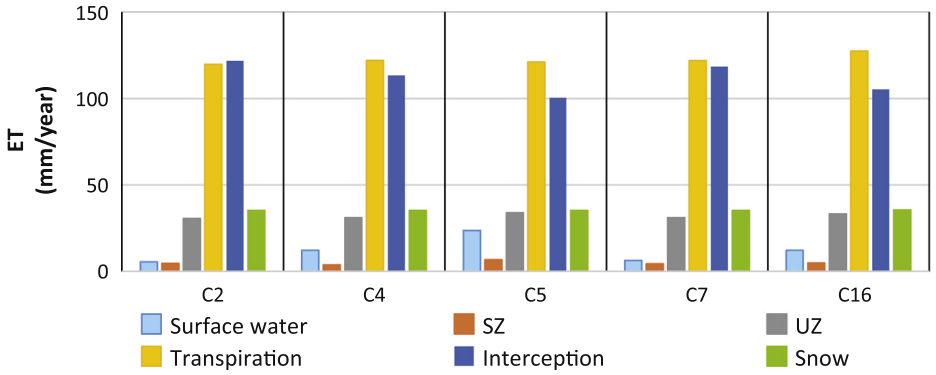

Fig. B2. Average ET contribution: Sub-catchments. Average annual simulated ET contributions for the sub-catchment representatives (2009–2014), Site C2, C4, C5, C7 and C16. In MSHE, water can evaporate as interception, transpiration, from surface waters (e.g. lakes), and from the saturated and unsaturated part of the soil. The results highlights results for the final model version, case 4e (2009-01-01 to 2015-01-01).

Table B1
Statistical results for the spring (Mar-May) during the calibration period (2009–01-01 to 2013–01-01). The results are for Case 1, Case 2, Case 3 and Case 4e for the sites C2, C4, C5, C7 and C16, and give their corresponding accumulated discharge errors and NSE values.

	Surface runoff error results, snowmelt period					
	Accumulated discharge error (%)			NSE		
	c. 2	c. 3	c. 4	c. 2	c. 3	c. 4
C2	−13	−15	−14	0.8	0.8	0.8
C4	12	−12	9	0.2	0.6	0.3
C5	−21	−41	−25	0.7	0.5	0.7
C7	3	−6	3	0.7	0.8	0.8
C16	−19	−26	−19	0.7	0.6	0.7

Table B2
Yearly accumulated discharge error results for each gauging station at Krycklan.

	2009	2010	2011	2012	2013	2014
C2	−4%	−8%	−32%	25%	15%	−15%
C4	9%	3%	−11%	8%	23%	−2%
C5	−27%	−26%	−39%	−17%	−6%	−25%
C7	11%	23%	9%	25%	38%	11%
C16	−10%	−11%	−10%	12%	11%	−16%
C1	22%	9%	9%	20%	33%	−11%
C6	−14%	−14%	−26%	8%	14%	−12%
C9	−1%	0%	−15%	1%	10%	−18%
C10	−2%	−10%	−36%	8%	−2%	−6%
C12	9%	34%	−6%	14%	24%	−10%
C13	1%	−3%	−25%	9%	9%	−1%
C14	30%	29%	−6%	42%	57%	35%
C15	−30%	−17%	−28%	0%	19%	−19%
C20	−20%	−22%	−46%	−7%	3%	−19%
Yearly average	−2%	−1%	−19%	10%	18%	−8%

Table B3
Observed and specific discharge (mm), evapotranspiration (ET) (mm) and precipitation (mm) for C2, C4, C5, C7 and C16. Observe that we have calculated the specific discharge values for all simulated days and for the days with observations, to enable comparison of model and observed results.

	Calibration period				Validation period		Average
C2	2009	2010	2011	2012	2013	2014	yr. 09–14
Observed specific discharge (mm)[1]	240	190	80	360	230	210	220
Calibrated specific discharge (mm)[1]	230	170	50	450	260	180	220
Calibrated specific discharge (mm)[2]	236	211	154	465	265	182	252
Precipitation (P) (mm)[2]	706	652	681	878	689	620	704
Evapotranspiration (ET) (mm)[2]	333	324	354	246	312	336	318
E/P (%)[2]	47.2	49.7	52.0	28.0	45.3	54.2	46.1
C4	2009	2010	2011	2012	2013	2014	yr. 09–14
Observed specific discharge (mm)[1]	310	270	280	570	350	350	360
Calibrated specific discharge (mm)[1]	340	280	250	608	430	340	375
Calibrated specific discharge (mm)[2]	409	361	300	608	430	340	408
Precipitation (P) (mm)[2]	706	652	681	878	689	620	704
Evapotranspiration (ET) (mm)[2]	334	324	354	246	313	336	318
E/P (%)[2]	47.3	49.7	52.0	28.0	45.4	54.2	46.1
C5	2009	2010	2011	2012	2013	2014	yr. 09–14
Observed specific discharge (mm)[1]	430	380	310	590	330	380	400
Calibrated specific discharge (mm)[1]	310	280	190	490	310	280	310
Calibrated specific discharge (mm)[2]	339	304	250	525	354	282	342
Precipitation (P) (mm)[2]	706	652	681	878	689	620	704
Evapotranspiration (ET) (mm)[2]	338	328	358	249	316	340	322
E/P (%)[2]	47.9	50.3	52.6	28.4	45.9	54.8	46.7
C7	2009	2010	2011	2012	2013	2014	yr. 09–14
Observed specific discharge (mm)[1]	320	280	260	480	300	290	320
Calibrated specific discharge (mm)[1]	350	346	280	596	409	319	383
Calibrated specific discharge (mm)[2]	380	346	280	596	409	319	388
Precipitation (P) (mm)[2]	706	652	681	878	689	620	704
Evapotranspiration (ET) (mm)[2]	334	324	354	246	312	336	318
E/P (%)[2]	47.3	49.7	52.0	28.0	45.3	54.2	46.1
C16	2009	2010	2011	2012	2013	2014	yr. 09–14
Observed specific discharge (mm)[1]	270	240	210	360	230	250	260
Calibrated specific discharge (mm)[1]	240	210	180	410	260	210	250
Calibrated specific discharge (mm)[2]	344	317	262	500	380	304	351
Precipitation (P) (mm)[2]	706	652	681	878	689	620	704
Evapotranspiration (ET) (mm)[2]	325	325	344	252	313	337	316
E/P (%)[2]	46.0	49.8	50.5	28.7	45.4	54.4	45.8

[1] Calculated value using simulated days for which there are observed data [2]Calculated value using all simulated days.

An estimation of how well the simulated groundwater heads correspond to the observed groundwater heads for every observation.

- Eq. C3 Mean absolute error (MAE)

$$MAE = \frac{1}{n}\sum_{t}|q_{obs_t} - q_{sim_t}|$$

An estimation of how well the simulated groundwater heads correspond to the observed water levels for every observation.

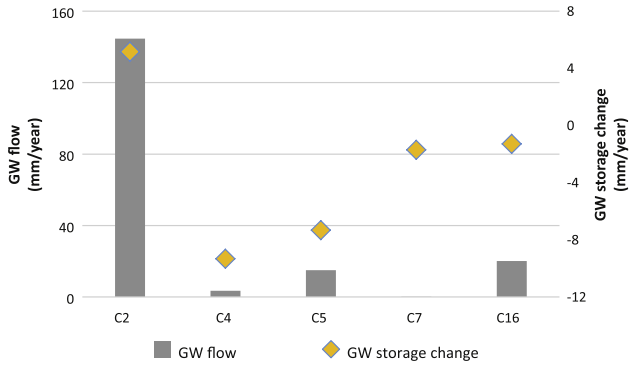

Fig. B3. Groundwater flow: Sub-catchments. Simulated average annual groundwater flow (GW flow) exiting from, without adding to river flow, for each sub-catchment representative, site C2, C4, C5, C7 and C16 as well as average annual groundwater storage change (GW storage change). The results highlights results for the final model version, case 4e (2009-01-01 to 2015-01-01).

- Eq. C4 Nash-Sutcliffe model efficiency (NSE)

$$R^2 = 1 - \frac{\sum_t (q_{obs_t} - q_{sim_t})^2}{\sum_t (q_{obs_t} - \overline{q}_{obs_t})^2}$$

An estimation on how well the simulated results correlate with observations. NSE can be $-\infty$ to 1, the closer to 1 the more accurate the model. If the value is negative, the mean of the observations is better for the prediction than the model.

- Eq. C5 Over/under-prediction of groundwater head in the model (β)

$$\beta = \frac{avergaeMEofallobs}{\Delta h_{max}}$$

$$\beta < 0.01 = \text{“}Highfidelity\text{”}$$

β expresses the full-scale model range under- or over-prediction in relation to the maximum observed global difference in groundwater headsΔh_{max}. If β is less than 0.01, the model is said to have “high fidelity”. It is recommended that β is considered together with ME, to account for the consideration that it is harder to achieve small ME values if the groundwater level heads changes rapidly over short distances due to large gradients.

References

Ågren, A.M., Lidberg, W., Strömgren, M., Ogilvie, J., Arp, P.A., 2014. Evaluating digital terrain indices for soil wetness mapping – a Swedish case study. Hydrol. Earth Syst. Sci. 18, 3623–3634. https://doi.org/10.5194/hess-18-3623-2014.

Alexandersson, H., 2003. Korrektion av nederbörd enligt enkel klimatologisk metodik. SMHI Meteorologi, Norrköping. 111.

Amvrosiadi, N., Seibert, J., Grabs, T., Bishop, K., 2017. Water storage dynamics in a till hillslope: the foundation for modeling flows and turnover times. Hydrol. Process. 31, 4–14. https://doi.org/10.1002/hyp.11046.

Andreassian, V., 2004. Waters and forests: from historical controversy to scientific debate. J. Hydrol. 291, 1–27. https://doi.org/10.1016/J.JHYDROL.2003.12.015.

Aneljung, M., Gustafsson, L., 2007. Sensitivity Analysis and Development of Calibration Methodology for Near-Surface Hydrogeology Model of Forsmark, SKB R-07-27. Svensk kärnbränslehantering AB, Stockholm.

Archfield, S.A., Vogel, R.M., 2010. Map correlation method: selection of a reference streamgage to estimate daily streamflow at ungaged catchments. Water Resour. Res. 46, 1–15. https://doi.org/10.1029/2009WR008481.

Bishop, K., Seibert, J., Nyberg, L., Rodhe, A., 2011. Water storage in a till catchment. II: implications of transmissivity feedback for flow paths and turnover times. Hydrol. Process. 25, 3950–3959. https://doi.org/10.1002/hyp.8355.

Bosson, E., Gustafsson, L.-G., Sassner, M., 2008. Numerical Modelling of Surface Hydrology and Near-Surface Hydrogeology at Forsmark-Site Descriptive Modelling. SDM-site Formark, SKB R-08-09. Svensk kärnbränslehantering AB, Stockholm.

Bosson, E., Sassner, M., Sabel, U., Gustafsson, L.-G., 2010. Modelling of Present and Future Hydrology and Solute Transport at Forsmark, SR-Site Biosphere, SKB R-10-02. Svensk kärnbränslehantering AB, Stockholm.

Bosson, E., Sabel, U., Gustafsson, L.G., Sassner, M., Destouni, G., 2012. Influences of shifts in climate, landscape, and permafrost on terrestrial hydrology. J. Geophys. Res. Atmos. 117, 1–12. https://doi.org/10.1029/2011JD016429.

Bosson, E., Selroos, J.-O., Stigsson, M., Gustafsson, L.-G., Destouni, G., 2013. Exchange and pathways of deep and shallow groundwater in different climate and permafrost conditions using the Forsmark site, Sweden, as an example catchment. Hydrogeol. J. 21, 225–237. https://doi.org/10.1007/s10040-012-0906-7.

Brooks, K.N., Ffolliott, P.F., Magner, J.A., 2012a. Groundwater and groundwater-surface water exchange. In: hydrology and the management of watersheds, pp. 173–195. doi:10.1016/B978-0-12-375674-9.10007-2.

Brooks, K.N., Folliott, P.F., Magner, J.A., 2012b. Infiltration, pathways of water flow and recharge. In: Hydrology and the Management of Watersheds. John Wiley & Sons, pp. 113–140. https://doi.org/10.1002/9781118459751.

Buffam, I., Laudon, H., Temnerud, J., Mörth, C.M., Bishop, K., 2007. Landscape-scale variability of acidity and dissolved organic carbon during spring flood in a boreal stream network. J. Geophys. Res. Biogeosci. 112, 1–11. https://doi.org/10.1029/2006JG000218.

Destouni, G., 2007. The subsurface water system role for surface and coastal water pollution. Ecohydrol. Hydrobiol. 7, 157–164. https://doi.org/10.1016/S1642-3593(07)70181-7.

Dogrul, E.C., Kadir, T.N., Brush, C.F., Chung, F.I., 2016. Linking groundwater simulation and reservoir system analysis models: the case for California's Central Valley. Environ. Model. Softw. 77, 168–182. 10.1016/j.envsoft.2015.12.006.

French, H.M., 2007. In: The Periglacial Environment. third ed. John Wiley & Sons Ltd.. https://doi.org/10.1002/9781118684931.

Goodrich, L.E., 1982. The influence of snow cover on the ground thermal regime. Can. Geotech. J. 19, 421–432. https://doi.org/10.1139/t82-047.

Grabs, T., Seibert, J., Bishop, K., Laudon, H., 2009. Modeling spatial patterns of saturated areas: a comparison of the topographic wetness index and a dynamic distributed model. J. Hydrol. 373, 15–23. 10.1016/j.jhydrol.2009.03.031.

Graham, D.N., Butts, M.B., 2005. Flexible integrated watershed modeling with MIKE SHE. Watershed model. 245–272. https://doi.org/10.1201/9781420037432.ch10.

Hardy, J.P., Groffman, P.M., Fitzhugh, R.D., Henry, K.S., Welman, A.T., Demers, J.D., Fahey, T.J., Driscoll, C.T., Tierney, G.L., Nolan, S., 2001. Snow depth manipulation and its influence on soil frost and water dynamics in a northern hardwood forest. Biogeochemistry 56, 151–174. https://doi.org/10.1023/A:1013036803050.

Hasselquist, E., Lidberg, W., RA., S., Ågren, A., Laudon, H., 2017. Identifying and assessing the potential hydrological function of past artificial forest drainage. AMBIO (in Press).

Hayashi, M., Quinton, W.L., Pietroniro, A., Gibson, J.J., 2004. Hydrologic functions of wetlands in a discontinuous permafrost basin indicated by isotopic and chemical signatures. J. Hydrol. 296, 81–97. https://doi.org/10.1016/j.jhydrol.2004.03.020.

Henriksen, H.J., Sonnenborg, T.O., 2005. In: Nøjagtighedskriterier Håndbog i grundvandsmodellering. Copenhagen. pp. 123–143.

Iwata, Y., Nemoto, M., Hasegawa, S., Yanai, Y., Kuwao, K., Hirota, T., 2011. Influence of rain, air temperature, and snow cover on subsequent spring-snowmelt infiltration into thin frozen soil layer in northern Japan. J. Hydrol. 401, 165–176. 10.1016/j.jhydrol.2011.02.019.

Johansson, E., Gustafsson, L.G., Berglund, S., Lindborg, T., Selroos, J.O., Claesson Liljedahl, L., Destouni, G., 2015. Data evaluation and numerical modeling of hydrological interactions between active layer, lake and talik in a permafrost catchment, Western Greenland. J. Hydrol. 527, 688–703. https://doi.org/10.1016/j.jhydrol.2015.05.026.

Kalbus, E., Reinstorf, F., Schirmer, M., 2006. Measuring methods for groundwater-surface water interactions: a review. Hydrol. Earth Syst. Sci. 10, 873–887. https://doi.org/10.5194/hess-10-873-2006.

Karlsen, R.H., Grabs, T., Bishop, K., Buffam, I., Laudon, H., Seibert, J., 2016a. Landscape controls on spatiotemporal discharge variability in a boreal catchment. Water Resour. Res. 52, 6541–6556. https://doi.org/10.1002/2016WR019186.

Karlsen, R.H., Seibert, J., Grabs, T., Laudon, H., Blomkvist, P., Bishop, K., 2016b. The assumption of uniform specific discharge: unsafe at any time? Hydrol. Process. 30, 3978–3988. https://doi.org/10.1002/hyp.10877.

Knutsson, G., Morfeldt, C.-O., 2002. Grundvatten. Teori & tillämpning. Svensk Byggtjänst, Solna.

Krause, P., Boyle, D.P., 2005. Advances in geosciences comparison of different efficiency criteria for hydrological model assessment. Adv. Geosci. 5, 89–97. https://doi.org/10.5194/adgeo-5-89-2005.

Kristensen, K.J., Jensen, S.E., 1975. A model for estimating actual evapotranspiration from potential evapotranspiration. Hydrol. Res. 6, 170–188.

Kuglerová, L., Jansson, R., Ågren, A., Laudon, H., Malm-Renöfält, B., 2014. Groundwater discharge creates hotspots of riparian plant species richness in a boreal forest stream network. Ecology 95, 715–725. https://doi.org/10.1890/13-0363.1.

Kuraś, P.K., Weiler, M., Alila, Y., 2008. The spatiotemporal variability of runoff generation and groundwater dynamics in a snow-dominated catchment. J. Hydrol. 352, 50–66. https://doi.org/10.1016/j.jhydrol.2007.12.021.

Laudon, H., 2004. Hydrological flow paths during snowmelt: congruence between hydrometric measurements and oxygen 18 in meltwater, soil water, and runoff. Water Resour. Res. 40, 1–9. https://doi.org/10.1029/2003WR002455.

Laudon, H., Ottosson Löfvenius, M., 2016. Adding snow to the picture – providing complementary winter precipitation data to the Krycklan catchment study database, s. 30, pp. 2413–2416, doi:10.1002/hyp.1075.

Laudon, H., Sponseller, R., 2017. How landscape organization and scale shape catchment hydrology and biogeochemistry: insights from a long-term catchment study. WIRE Water (In Press).

Laudon, H., Sjöblom, V., Buffam, I., Seibert, J., Mörth, M., 2007. The role of catchment scale and landscape characteristics for runoff generation of boreal streams. J. Hydrol. 344, 198–209. https://doi.org/10.1016/j.jhydrol.2007.07.010.

Laudon, H., Taberman, I., Ågren, A., Futter, M., Ottosson-Löfvenius, M., Bishop, K., 2013. The Krycklan catchment study – a flagship infrastructure for hydrology, biogeochemistry, and climate research in the boreal landscape. Water Resour. Res. 49, 7154–7158. https://doi.org/10.1002/wrcr.20520.

Lidman, F., Ramebäck, H., Bengtsson, Å., Laudon, H., 2013. Distribution and transport of radionuclides in a boreal mire – assessing past, present and future accumulation of uranium, thorium and radium. J. Environ. Radioact. 121, 87–97. https://doi.org/10.1016/j.jenvrad.2012.06.010.

Lindgren, G.A., Destouni, G., Miller, A.V., 2004. Solute transport through the integrated groundwater-stream system of a catchment. Water Resour. Res. 40. https://doi.org/10.1029/2003WR002765.

McNamara, J.P., Kane, D.L., Hinzman, L.D., 1997. Hydrograph separations in an arctic watershed using mixing model and graphical techniques. Water Resour. Res. 33, 1707–1719. https://doi.org/10.1029/97WR01033.

Metcalfe, R.A., Buttle, J.M., 2001. Soil partitioning and surface store controls on spring runoff from a boreal forest peatland basin in north-central Manitoba. Can. Hydrol. Process. 15, 2305–2324. https://doi.org/10.1002/hyp.262.

Nippgen, F., McGlynn, B.L., Marshall, L.A., Emanuel, R.E., 2011. Landscape structure and climate influences on hydrologic response. Water Resour. Res. 47. https://doi.org/10.1029/2011WR011161.

Niu, G.-Y., Yang, Z.-L., 2006. Effects of frozen soil on snowmelt runoff and soil water storage at a continental scale. J. Hydrometeorol. 7, 937–952. https://doi.org/10.1175/JHM538.1.

Nyberg, L., Sthli, M., Mellander, P.E., Bishop, K.H., 2001. Soil frost effects on soil water and runoff dynamics along a boreal forest transect: 1. field investigations. Hydrol. Process. https://doi.org/10.1002/hyp.256.

Oni, S.K., Tiwari, T., Ledesma, J.L.J., Ågren, A.M., Teutschbein, C., Schelker, J., Laudon, H., Futter, M.N., 2015. Local- and landscape-scale impacts of clear-cuts and climate change on surface water dissolved organic carbon in boreal forests. J. Geophys. Res. Biogeosci. 120, 2402–2426. https://doi.org/10.1002/2015JG003190.

Oni, S.K., Mieres, F., Futter, M.N., Laudon, H., 2017. Soil temperature responses to climate change along a gradient of upland-riparian transect in boreal forest. Clim. Change 143, 27–41. https://doi.org/10.1007/s10584-017-1977-1.

Orradottir, B., Archer, S.R., Arnalds, O., Wilding, L.P., Thurow, T.L., 2008. Infiltration in Icelandic andisols: the role of vegetation and soil frost. Arct. Antarct. Alp. Res. 40, 412–421.

Payn, R.A., Gooseff, M.N., McGlynn, B.L., Bencala, K.E., Wondzell, S.M., 2012. Exploring changes in the spatial distribution of stream baseflow generation during a seasonal recession. Water Resour. Res. 48. https://doi.org/10.1029/2011WR011552.

Peralta-Tapia, A., Sponseller, R.A., Tetzlaff, D., Soulsby, C., Laudon, H., 2015. Connecting precipitation inputs and soil flow pathways to stream water in contrasting boreal catchments. Hydrol. Process. 29, 3546–3555. https://doi.org/10.1002/hyp.10300.

Rodhe, A., Seibert, J., 1999. Wetland occurrence in relation to topography: a test of topographic indices as moisture indicators. Agric. For. Meteorol. 98–99, 325–340. https://doi.org/10.1016/S0168-1923(99)00104-5.

Sivapalan, M., 2003. Process complexity at hillslope scale, process simplicity at the watershed scale: is there a connection? Hydrol. Process. 17, 1037–1041. https://doi.org/10.1002/hyp.5109.

Sophocleous, M., 2002. Interactions between groundwater and surface water: the state of the science. Hydrogeol. J. 10, 52–67. https://doi.org/10.1007/s10040-001-0170-8.

Tiwari, T., Buffam, I., Sponseller, R.A., Laudon, H., 2017. Inferring scale-dependent processes influencing stream water biogeochemistry from headwater to sea. Oceanogr. Limnol. 10.1002/lno.10738.

Woo, M.-K., 2012. In: Permafrost Hydrology. Springer, Berlin Heidelberg. https://doi.org/10.1007/978-3-642-23462-0.

Woods, R., 2006. Hydrologic concepts of variability and scale. In: Encyclopedia of Hydrological Sciences. John Wiley & Sons, Ltd.. https://doi.org/10.1002/0470848944.hsa002.

Wu, L.Z., Selvadurai, A.P.S., 2016. Rainfall infiltration-induced groundwater table rise in an unsaturated porous medium. Environ. Earth Sci. 75, 135. https://doi.org/10.1007/s12665-015-4890-9.

Yang, J., McMillan, H., Zammit, C., 2017. Modeling surface water–groundwater interaction in New Zealand: model development and application. Hydrol. Process. 31, 925–934. https://doi.org/10.1002/hyp.11075.

Zimmer, M.A., McGlynn, B.L., 2017. Bidirectional stream-groundwater flow in response to ephemeral and intermittent streamflow and groundwater seasonality. Hydrol. Process. 31, 3871–3880. https://doi.org/10.1002/hyp.11301.